JFM RAPIDS
journals.cambridge.org/rapids

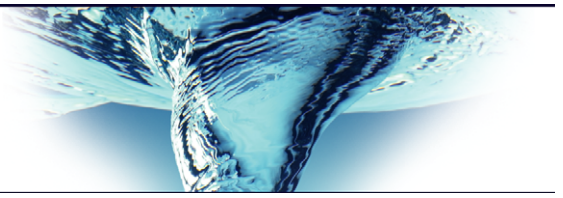

Localized edge states in the asymptotic suction boundary layer

T. Khapko[1,†], T. Kreilos[2,3], P. Schlatter[1], Y. Duguet[4], B. Eckhardt[2,5] and D. S. Henningson[1]

[1]Linné FLOW Centre, KTH Mechanics, Royal Institute of Technology, SE-100 44 Stockholm, Sweden

[2]Fachbereich Physik, Philipps-Universität Marburg, D-35032 Marburg, Germany

[3]Max Planck Institute for Dynamics and Self-Organization, D-37077 Göttingen, Germany

[4]LIMSI-CNRS, UPR 3251, Université Paris-Sud, F-91403, Orsay, France

[5]J. M. Burgerscentrum, Delft University of Technology, NL-2628 CD Delft, The Netherlands

(Received 12 November 2012; revised 17 December 2012; accepted 4 January 2013; first published online 7 February 2013)

The dynamics on the laminar–turbulent separatrix is investigated numerically for boundary-layer flows in the subcritical regime. Constant homogeneous suction is applied at the wall, resulting in a parallel asymptotic suction boundary layer (ASBL). When the numerical domain is sufficiently extended in the spanwise direction, the coherent structures found by edge tracking are invariably localized and their dynamics shows bursts that drive a remarkable regular or irregular spanwise dynamics. Depending on the parameters, the asymptotic dynamics on the edge can be either periodic in time or chaotic. A clear mechanism for the regeneration of streaks and streamwise vortices emerges in all cases and is investigated in detail.

Key words: boundary layers, instability, nonlinear dynamical systems

1. Introduction

Near-wall coherent structures such as streaks and quasi-streamwise vortices are a ubiquitous feature of transitional and turbulent wall-bounded shear flows. Their regeneration process is intimately connected with the occurrence of *bursting* events, i.e. strong intermittent ejections of low-speed fluid from the wall (for a review see e.g Robinson 1991). Classical linear stability theory applied to the base profiles of the various canonical wall-bounded flows predicts spanwise independent modes, so-called Tollmien–Schlichting waves, as the most unstable disturbances (see e.g. Schmid & Henningson 2001). As evidenced by numerous experiments and simulations, these

† Email address for correspondence: taras@mech.kth.se

doi:10.1017/jfm.2013.20

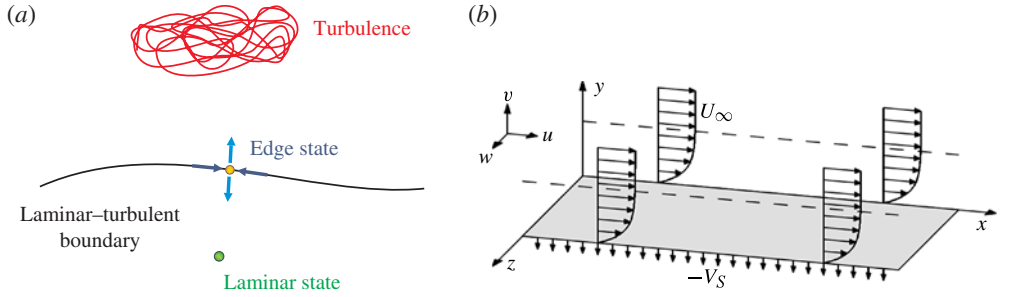

FIGURE 1. (*a*) Conceptual two-dimensional sketch of the state space. The turbulent and laminar states are shown in red and green, respectively. The separatrix (black line) supports the edge state (yellow circle), which is attracting within the boundary and repelling in a direction transverse to it. (*b*) Sketch of the asymptotic suction boundary layer (ASBL), where constant homogeneous suction is applied at the wall. Figure adapted from Levin & Henningson (2007).

waves are not relevant in the context of sustaining near-wall turbulence. In the case of a spatially developing Blasius boundary layer, the laminar base flow is linearly stable up to a finite value of the Reynolds number Re, where $Re_c \approx 520$ based on the displacement thickness (see e.g. Schlichting 1987). However, in the presence of strong noise, subcritical transition may occur as well further upstream via the formation of streamwise streaks, bypassing the classical transition scenario (see e.g. Brandt, Schlatter & Henningson 2004). These elongated structures appear as a result of the large sensitivity to forcing and large transient energy growth of these structures in shear flows (Schmid & Henningson 2001). Thus streamwise streaks and streamwise vortices can also be observed for boundary-layer flows in the absence of any linear instability of the base flow. Such coherent structures seem closely connected with the finite-amplitude solutions encountered in studies of subcritical transition in channels (Itano & Toh 2001; Jiménez *et al.* 2005).

We will hence focus here on coherent structures as well as bursting events in the framework of subcritical transition only. A recent idea specific to subcritical instabilities is to analyse the laminar–turbulent separatrix, the invariant phase-space region separating trajectories that relaminarize from those experiencing turbulent dynamics (Itano & Toh 2001). Relative attractors on this separatrix are called edge states (Skufca, Yorke & Eckhardt 2006). They correspond to an (unstable) equilibrium regime and are thus crucial for: (i) understanding the structure of the phase space; and (ii) identifying the physical mechanisms by which the flow can sustain non-trivial dynamics. The concept of edge states has been developed in studies of cylindrical Poiseuille flow and plane Couette flow, which both admit simple laminar solutions that are linearly stable for all Reynolds numbers Re. However, in practice another concurrent flow regime, namely turbulence, can be observed for moderate values of Re, depending on the shape and amplitude of the initial perturbation to the laminar base flow. There is compelling evidence that trajectories restricted to the laminar–turbulent separatrix are attracted towards the edge state (see figure 1*a*), which can be either a fixed point (Schneider *et al.* 2008), a travelling wave (Duguet, Willis & Kerswell 2008), a relative periodic orbit (Toh & Itano 2003) or even a chaotic object (Schneider, Eckhardt & Yorke 2007). These pioneering investigations of edge states were performed numerically in the context of minimal flow units (Jiménez

& Moin 1991; Hamilton, Kim & Waleffe 1995). Later investigations in extended computational domains (Duguet, Schlatter & Henningson 2009; Mellibovsky *et al.* 2009; Schneider, Marinc & Eckhardt 2010) revealed robust spatial localization for the edge state, indicating a connection to incipient turbulent spots (Henningson, Spalart & Kim 1987; Lundbladh & Johansson 1991), puffs and slugs (Duguet, Willis & Kerswell 2010).

The concept of edge states was recently carried over to the Blasius boundary-layer flow over a flat plate (Cherubini *et al.* 2011; Duguet *et al.* 2012), where an additional complication is the spatial development of the boundary layer. Duguet *et al.* (2012) have identified almost-cyclic dynamics on the edge in terms of rescaled variables, where the rescaling is done with respect to the local boundary-layer thickness. Edge tracking in a spatially inhomogeneous context, however, is computationally demanding, as the proper asymptotic dynamics remains currently out of reach in a numerical domain of finite streamwise extent. Parallel flows are much better suited to asymptotic edge tracking since periodic boundary conditions allow for both streamwise periodic structures and a constant layer thickness (i.e. Reynolds number) in the domain.

Hence we focus here on a parallel model for boundary layers, for which a number of variants have been discussed in the literature. Spalart & Yang (1987) proposed a model for a temporal boundary layer in a moving frame of reference, which implies a homogeneous boundary-layer thickness throughout the domain, which slowly grows in time. Another approach was developed by Spalart (1988) and recently used with some modification in an edge tracking study (Biau 2012). In their model a multi-scale approximation of the flow was used to simulate the temporal evolution of a fixed short streamwise portion of the boundary layer. In this paper we will focus on a third alternative: suction is applied at the lower wall to compensate for the spatial growth of the laminar profile. In the case when the suction is constant and homogeneous, the boundary-layer thickness rapidly saturates and the associated flow is termed asymptotic suction boundary layer (ASBL). Studying transition to turbulence in ASBL bears considerable advantages: (i) its laminar solution is independent of the streamwise position; (ii) it is one of the canonical solutions of the incompressible Navier–Stokes equations (Schlichting 1987); (iii) the laminar solution is linearly stable for a wide range of values of Re; and (iv) it is realizable in wind-tunnel experiments using a porous plate with well-controlled suction. Applying suction is a powerful technique for flow control, hence ASBL has been the subject of a number of numerical (Mariani *et al.* 1993; Levin & Henningson 2007; Schlatter & Örlü 2011) and experimental studies (Antonia *et al.* 1988; Fransson & Alfredsson 2003).

A numerical characterization of the edge states in ASBL is the main focus of this paper. The structure of the paper is as follows. Parameters and numerical technique are described in § 2. The results of edge tracking are presented in § 3 for both a minimal flow unit and a spanwisely extended domain, where the spatial localization and dynamics will be scrutinized. The main conclusions are given in the final section.

2. Problem set-up and numerical methodology

ASBL is the flow above a permeable flat plate subject to constant homogeneous suction (see figure 1*b*). The incompressible Navier–Stokes equations admit in this case a laminar solution where the velocity field is independent of the streamwise position x,

$$U = U_\infty(1 - \mathrm{e}^{-yV_S/\nu}), \quad V = -V_S. \tag{2.1}$$

Here y is the wall-normal distance from the plate, $\boldsymbol{U} = (U, V)$ is the velocity field of the base flow in the streamwise and wall-normal (x, y) directions, U_∞ and V_S are the imposed free stream and suction velocities, respectively, and ν is the fluid kinematic viscosity. An expression for the laminar displacement thickness δ^* can be found analytically as

$$\delta^* = \int_0^\infty (1 - u(y)/U_\infty)\,\mathrm{d}y = \frac{\nu}{V_S}. \tag{2.2}$$

The Reynolds number based on δ^* is defined by $Re = U_\infty \delta^*/\nu = U_\infty/V_S$. The laminar solution is linearly stable for Reynolds numbers up to $Re_c = 54\,370$ (Hocking 1975); however, transition to turbulence can be observed already above $Re \approx 300$ (Schlatter & Örlü 2011).

Numerical simulations of the ASBL are performed here with a fully spectral method, which solves the unsteady incompressible Navier–Stokes equations in a domain $\Omega = [-L_x/2, L_x/2] \times [0, L_y] \times [-L_z/2, L_z/2]$. The velocity field $\boldsymbol{u} = (u, v, w)$ is expanded using N_x and N_z Fourier modes in the streamwise x and spanwise z directions, respectively, and N_y Chebyshev polynomials in the wall-normal y direction. Hence, periodicity is imposed in both x and z. In the wall-normal direction, Dirichlet boundary conditions are used at both ends of the domain,

$$(u, v, w)_{y=0} = (0, -V_S, 0), \tag{2.3a}$$

$$(u, v, w)_{y=L_y} = (U_\infty, -V_S, 0). \tag{2.3b}$$

Dealiasing with the 3/2 rule is performed in the x and z directions. The results were validated by comparison between two codes – SIMSON (Chevalier *et al.* 2007) and ChannelFlow (Gibson 2012). For time advancement, third-order Runge–Kutta and second-order Crank–Nicolson methods are used for the nonlinear and linear terms, respectively, with SIMSON, and a third-order semi-implicit backward differentiation scheme with ChannelFlow. We have verified that both codes lead to the same results and the same edge states both qualitatively and quantitatively. We therefore only present results obtained with SIMSON in this paper. Non-dimensionalization with U_∞ and δ^* is used throughout the paper. One has to be careful when choosing the height L_y of the numerical domain, since the boundary layer tends to become very thick for turbulent ASBL (Schlatter & Örlü 2011), saturating at very high values of 99 % velocity thickness δ_{99} compared to the laminar case. However, δ_{99} for edge states is much lower, and $L_y = 15$ proved sufficient for the present investigation. Edge tracking was performed in two different distinct set-ups. In the first case, which we refer to as a minimal flow unit, the domain has size $(L_x, L_y, L_z) = (10, 15, 6)$, with a numerical resolution of $N_x \times N_y \times N_z = 32 \times 129 \times 32$ spectral modes. In the second case, the numerical domain is extended in the spanwise direction to a size of $(L_x, L_y, L_z) = (6\pi, 15, 50)$, with the corresponding resolution $N_x \times N_y \times N_z = 48 \times 129 \times 192$. The results presented here were obtained for $Re = 500$. Lowering Re to 400 did not show any significant changes in the dynamics. Resolution checks were performed for the key simulations by doubling the number of spectral modes in each direction. It turns out that the chosen resolution is fully adequate for edge states and the early transitional stages, while higher resolution and larger values for L_y are needed for the turbulent state to be accurately captured.

The dynamics on the separatrix is tracked using the bisection technique described by Skufca *et al.* (2006). A set of initial conditions $\boldsymbol{u}_\lambda = \boldsymbol{U} + \lambda(\boldsymbol{u}_0 - \boldsymbol{U})$ is considered, where $\boldsymbol{u}_0$ is an arbitrary non-trivial flow state. Initial conditions corresponding to

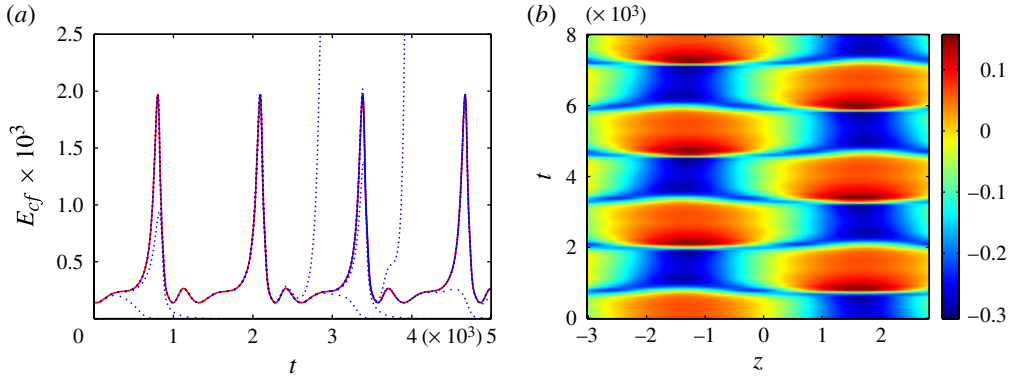

FIGURE 2. (*a*) Evolution of the cross-flow energy E_{cf} with time t for the edge state in a minimal flow unit. The solid red line corresponds to the converged edge trajectory, whereas dotted blue lines correspond to trajectories diverging from the edge. (*b*) Space–time diagram for the streamwise velocity fluctuations u' averaged in x at $y = 1$ corresponding to the edge state in the minimal flow unit.

various values of λ are evolved in time until they approach either the laminar or the turbulent state, according to the predefined thresholds for the root-mean-square (r.m.s.) value of the wall-normal velocity fluctuations v_{rms}. By iteratively bisecting the value of λ, we bracket the laminar–turbulent boundary and obtain a trajectory that evolves for a sufficiently long time without becoming either laminar or turbulent. Because of the exponential separation of initially nearby trajectories and the limited numerical accuracy of the bisection, the resulting trajectory visits the boundary for a finite time only. However, by restarting the bisection from the last state closest to the edge often enough, it is possible to stay on the edge for an infinite time and to reach a relative attractor.

3. Edge states

3.1. *Minimal flow unit*

The edge state in small computational domains close to a minimal flow unit has been discussed by Kreilos *et al.* (2012). We briefly summarize the key features of the edge state in a box of size $(L_x, L_y, L_z) = (10, 15, 6)$.

The time evolution of the cross-flow energy based on the wall-normal $v' = v - V$ and spanwise $w' = w$ velocity fluctuations of this state,

$$E_{cf} = \frac{1}{L_x L_z \delta^*} \int_\Omega (v'^2 + w'^2)\, \mathrm{d}x\, \mathrm{d}y\, \mathrm{d}z, \tag{3.1}$$

is shown in figure 2(*a*). This quantity measures the energy in the components transverse to the downstream flow and captures the intensity of the vortices. We see that there are long phases in which E_{cf} changes only slowly, followed by strong bursts at regular time intervals. Figure 2(*b*) shows the downstream velocity fluctuations $u' = u - U$ averaged in x at $y = 1$. We see that, during the calm phase, the state consists of a low- and a high-speed streak. At each burst, the low-speed streak is broken up into two parts, which reconnect across the periodic boundaries to form a

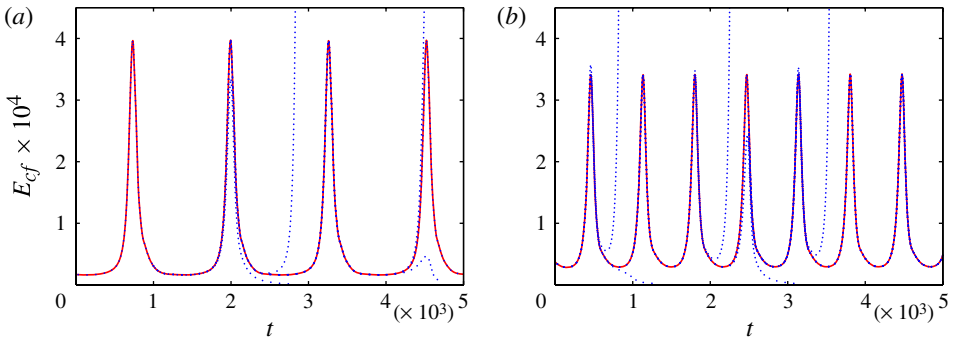

FIGURE 3. Time evolution of the cross-flow energy: (*a*) L edge state (indiscernible from R state); (*b*) LR state. The colour coding is the same as in figure 2(*a*). See the text for the definition of L, R and LR states.

new low-speed streak at a position that is shifted by half the box width. The edge state is hence a periodic orbit with a period that is twice the interval between bursts, i.e. 2×1290. A homotopy between plane Couette flow and ASBL was suggested by Kreilos *et al.* (2012) to explain the bifurcation underlying the bursts and the shifts: on the path from plane Couette flow to ASBL, the periodic orbit emerges from a saddle-node infinite-period (SNIPER) bifurcation undergone by two symmetry-related pairs of travelling waves.

3.2. *Spanwise localized edge states*

The dynamics described above relies heavily on the spanwise periodicity imposed by the value of L_z, which is comparable to the streak spacing. In this work, we want to investigate the dynamics of the edge state in the absence of interaction with its periodic copies. We thus extend the spanwise width of the computational box to $L_z = 50$ while keeping L_x relatively low at 6π. As in the minimal flow unit, the cross-flow energy of the edge state is found to be periodic in time. By varying the initial perturbation $\boldsymbol{u}_0$ used for edge tracking, we obtain not one, but three states. Two of them are actually related by $z \leftarrow z_0 - z$ transformations, under which the system with boundary conditions (2.3) is invariant (z_0 is arbitrary). The time evolution of the cross-flow energy for all these states is shown in figure 3. Despite the difference in the periods, the edge trajectories all show similar characteristics to the small box case, i.e. a periodic alternation of calm phases and bursts. Space–time diagrams for $\langle u' \rangle_x(y = 1)$ shown in figure 4(*a–c*) reveal a clear spanwise localization of the kinetic energy, as in former studies of edge states in other systems (Schneider *et al.* 2010). This localization property is robust to variations in L_z, as attested by figure 5(*a*).

The structure and dynamics of the three edge states can be understood from the space–time diagrams in figure 4(*a–c*). The velocity fields are dominated by a pair of high- and low-speed streaks, which undergo a burst in cross-flow energy before being shifted in the spanwise direction. Depending on the direction of the shift, we distinguish between the two symmetry-related states that repeatedly hop towards the right (R) or towards the left (L), and the state that alternates regularly between hopping left and right (LR). As already mentioned, the L and R states differ in the direction of the shifts but otherwise have exactly the same characteristics since they

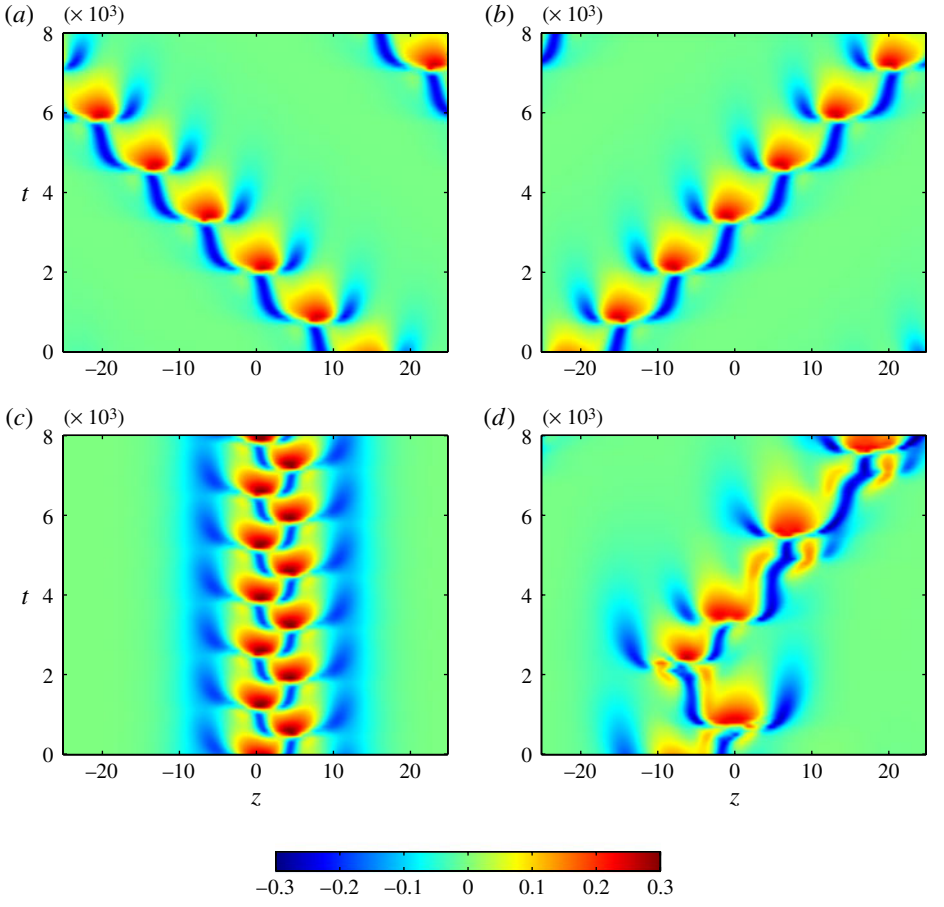

FIGURE 4. Space–time diagrams for streamwise velocity fluctuations u' averaged in x at $y = 1$: (*a*) left-going state (L); (*b*) right-going state (R); (*c*) alternate left- and right-going state (LR); (*d*) chaotic edge state for $L_x = 4\pi$.

are related by a reflection symmetry. The period between two bursts of the LR state is approximately 668, while that for both L and R states is 1263, hence a bit shorter than twice the LR period.

Though we distinguish between two fundamental states based on the different motions in the spanwise direction z, the qualitative dynamics between two consecutive bursts appears to be similar in all three cases. Therefore, our analysis of the detailed sequence of events during one period can be limited to one of these states only. In the following, we focus on the left-hopping state (L). Key snapshots of the cycle are shown in figure 6; supplementary movies are available at http://dx.doi.org/10.1017/jfm.2013.20. Starting from the calm phase, the state consists of one high-speed streak with two low-speed streaks on each side. One of the low-speed streaks is moderately bent and is flanked by counter-rotating quasi-streamwise vortices. These vortices induce upward motion that advects slow fluid away from the wall, explaining the presence of the low-speed streak (lift-up effect). Conversely, the second streak is less bent and

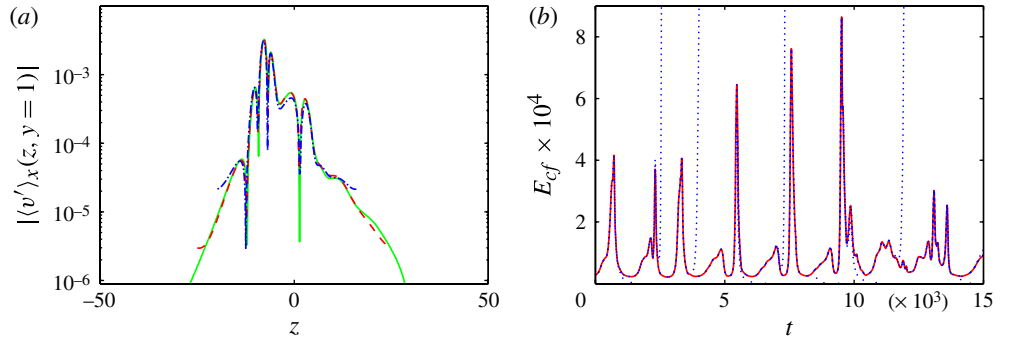

FIGURE 5. (*a*) Absolute value of the wall-normal velocity fluctuations averaged in x at $y = 1$ evaluated at the time between two bursts for the L state with various spanwise widths of the domain: ———, $L_z = 100$; – – – –, $L_z = 50$; —·—, $L_z = 36$. (*b*) Time evolution of the cross-flow energy E_{cf} for one of the edge trajectories in the shorter domain $L_x = 4\pi$. The colour coding is the same as in figure 2(*a*).

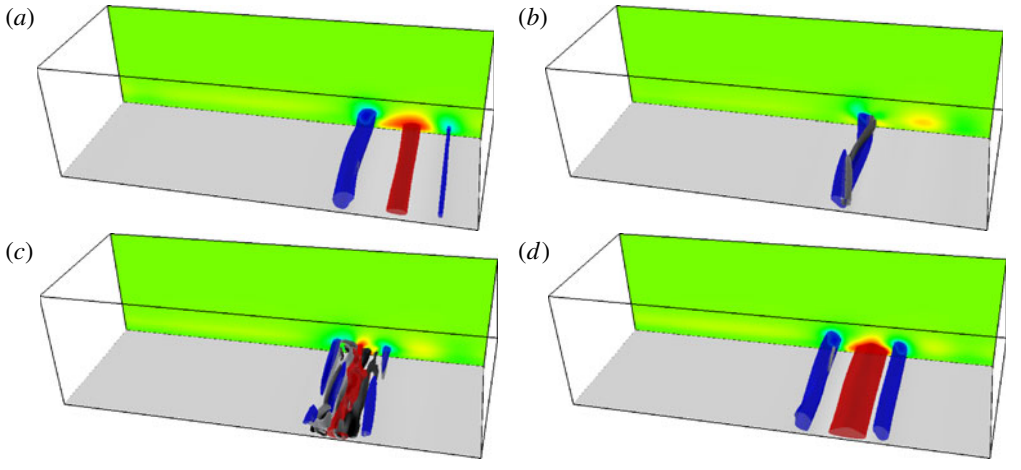

FIGURE 6. Three-dimensional visualization during one period of the L state. Isosurfaces of streamwise velocity fluctuations $u' = \pm 0.15$ are coloured in blue (low-speed streak) and red (high-speed streak), respectively. Vortices are visualized using the λ_2 criterion (Jeong & Hussain 1995), with the isosurface $\lambda_2 = -0.001$ coloured by the streamwise vorticity (grey-scale). The whole computational domain is shown. (*a*) High-speed streak with two low-speed streaks on the side during the calm phase at $t = 2500$. (*b*) Strong quasi-streamwise vortices that lean over the active low-speed streak at $t = 3100$. (*c*) Breakdown at $t = 3300$. (*d*) Initial structures regenerated with a shift in the spanwise direction at $t = 3470$. Supplementary movies for the L state as well as the LR state are available at http://dx.doi.org/10.1017/jfm.2013.20.

is slowly decaying. As the vortices grow in strength, they wrap around the streak, tilting in the streamwise direction and causing the streak to bend even further. At some point the tips of the vortices cross the bent streak, each of them dividing the streak into two regions with respect to its streamwise extent. In the first region the vortex is still sustaining the streak, while in the second one it pushes fluid down instead of

lifting it up. As the vortices cross the streak, they also cross each other, enhancing the push-down effect and ultimately leading to the breakdown of the low-speed streak and creation of a high-speed streak at the same location. During the same time, the other low- and high-speed streaks decay. Those events correspond to the burst in the cross-flow energy. In the streak breakdown process, the initial streamwise vortices are destroyed and new vortices are re-created in the area around the newly created high-speed streak. The vortices on both sides of the high-speed streak create two low-speed streaks and the loop is closed. The low-speed streak on the left is the active one that will develop instabilities and break down during the next burst, while the right one will slowly decay, resulting in a leftwards shift of the whole structure.

This self-sustaining process resembles the regeneration cycle of the near-wall turbulent structures discussed by Hamilton *et al.* (1995). We also start with streaks, one of which develops an instability leading to its streamwise modulation (x-dependent flow in the work by Hamilton *et al.* (1995)). In the process of streak breakdown, new vortices are created, which corresponds to the vortex regeneration phase. Finally, the streamwise vortices re-create the streaks by linear advection and return to the beginning of the cycle. A distinct feature of the process in ASBL is the spanwise shift of the regenerated streaks, which was not an intrinsic part of the self-sustaining process by Hamilton *et al.* (1995).

One of the most important parts of the dynamics – vortices crossing the streak – was also suggested in near-wall turbulence in minimal units (Jiménez & Moin 1991) and later confirmed using feature eduction in extended domains (Jeong *et al.* 1997). Similar structures are also observed in boundary layers during bypass transition (Schlatter *et al.* 2008). The same mechanism can also be identified in the small box ASBL (Kreilos *et al.* 2012), albeit the two low-speed streaks created after the burst correspond to the same streak in this case owing to the small box periodicity.

3.3. *Chaotic behaviour of the localized edge state*

As the domain length is decreased to 4π, the periodicity of all three edge states is lost. The resulting dynamics on the edge is chaotic, though also consisting of calm and bursting regions (see figure 5*b*). In figure 4(*d*) we present the space–time diagram corresponding to one of the edge trajectories in this case. We see that the structures remain localized and that the bursts in the cross-flow energy still correspond to hops in the spanwise direction. However, the direction and the distance of those shifts is no longer fixed but varies in an unpredictable fashion.

Insights into the transition from the periodic to the aperiodic behaviour can be obtained by slowly lowering the parameter L_x from 6π towards 4π. We find that the periodic behaviour is sustained at least down to $L_x = 5\pi$, below which new states – with longer periods and more complex sequences of spanwise shifts – emerge as attractors. These bifurcations indicate that the periodic solutions discussed above acquire at least one more unstable direction, hence cannot serve as relative attractors any longer and can only be visited transiently by the edge trajectories (Duguet *et al.* 2008). Nevertheless, they may still constitute the beginning of a symbolic dynamics for the chaotic regime. The complete cascade of bifurcations leading from periodic towards chaotic edge states is currently under investigation.

4. Conclusions

To summarize, we have tracked the dynamics on the laminar–turbulent separatrix in the asymptotic suction boundary layer, which turns out always to be localized in

wide enough domains. We were able to identify a robust cycle encompassing a calm phase with slow growth of a sinuous-type instability on a low-speed streak, and a violent burst of the streak due to vortex interaction once they are crossing the streak. Regeneration of new quasi-streamwise vortices and low-speed streaks accompanied by a spanwise shift closes the cycle. This mechanism bears many similarities to processes previously discussed in the context of minimal channel flow and the near-wall regeneration cycle in wall-bounded turbulence (Jiménez & Moin 1991; Hamilton *et al.* 1995; Jiménez *et al.* 2005). Depending on the streamwise length of the domain used in the simulations, imposing the wavelength of the instability, the edge dynamics can be regular or erratic. This suggests the existence of periodic orbits on the edge which behave as attractors or saddle points. A more detailed study of the effects of the streamwise localization and the relevance of the identified bursting dynamics for both laminar–turbulent transition and fully developed near-wall turbulence are currently under investigation.

Acknowledgement

Computer time provided by SNIC (Swedish National Infrastructure for Computing) is gratefully acknowledged.

Supplementary movies

Supplementary movies are available at http://dx.doi.org/10.1017/jfm.2013.20.

References

ANTONIA, R. A., FULACHIER, L., KRISHNAMOORTHY, L. V., BENABID, T. & ANSELMET, F. 1988 Influence of wall suction on the organized motion in a turbulent boundary layer. *J. Fluid Mech.* **190**, 217–240.

BIAU, D. 2012 Laminar–turbulent separatrix in a boundary layer flow. *Phys. Fluids* **24**, 034107.

BRANDT, L., SCHLATTER, P. & HENNINGSON, D. S. 2004 Transition in boundary layers subject to free-stream turbulence. *J. Fluid Mech.* **517**, 167–198.

CHERUBINI, S., DE PALMA, P., ROBINET, J. C. & BOTTARO, A. 2011 Edge states in a boundary layer. *Phys. Fluids* **23**, 051705.

CHEVALIER, M., SCHLATTER, P., LUNDBLADH, A. & HENNINGSON, D. S. 2007 A pseudo-spectral solver for incompressible boundary layer flows. *Tech. Rep.* TRITA-MEK 2007:07. KTH Mechanics, Stockholm, Sweden.

DUGUET, Y., SCHLATTER, P. & HENNINGSON, D. S. 2009 Localized edge states in plane Couette flow. *Phys. Fluids* **21**, 111701.

DUGUET, Y., SCHLATTER, P., HENNINGSON, D. S. & ECKHARDT, B. 2012 Self-sustained localized structures in a boundary-layer flow. *Phys. Rev. Lett.* **108**, 044501.

DUGUET, Y., WILLIS, A. P. & KERSWELL, R. R. 2008 Transition in pipe flow: the saddle structure on the boundary of turbulence. *J. Fluid Mech.* **613**, 255–274.

DUGUET, Y., WILLIS, A. P. & KERSWELL, R. R. 2010 Slug genesis in cylindrical pipe flow. *J. Fluid Mech.* **663**, 180–208.

FRANSSON, J. H. M. & ALFREDSSON, P. H. 2003 On the disturbance growth in an asymptotic suction boundary layer. *J. Fluid Mech.* **482**, 51–90.

GIBSON, J. F. 2012 ChannelFlow: a spectral Navier–Stokes simulator in C++. *Tech. Rep*. University of New Hampshire, http://channelflow.org.

HAMILTON, J. M., KIM, J. & WALEFFE, F. 1995 Regeneration mechanisms of near-wall turbulence structures. *J. Fluid Mech.* **287**, 317–348.

HENNINGSON, D. S., SPALART, P. R. & KIM, J. 1987 Numerical simulations of turbulent spots in plane Poiseuille and boundary-layer flow. *Phys. Fluids* **30**, 2914–2917.

HOCKING, L. M. 1975 Non-linear instability of the asymptotic suction velocity profile. *Q. J. Mech. Appl. Maths* **28** (3), 341–353.

ITANO, T. & TOH, S. 2001 The dynamics of bursting process in wall turbulence. *J. Phys. Soc. Japan* **70**, 703–716.

JEONG, J. & HUSSAIN, F. 1995 On the identification of a vortex. *J. Fluid Mech.* **285**, 69–94.

JEONG, J., HUSSAIN, F., SCHOPPA, W. & KIM, J. 1997 Coherent structures near the wall in a turbulent channel flow. *J. Fluid Mech.* **332**, 185–214.

JIMÉNEZ, J., KAWAHARA, G., SIMENS, M. P., NAGATA, M. & SHIBA, M. 2005 Characterization of near-wall turbulence in terms of equilibrium and 'bursting' solutions. *Phys. Fluids* **17**, 015105.

JIMÉNEZ, J. & MOIN, P. 1991 The minimal flow unit in near-wall turbulence. *J. Fluid Mech.* **225**, 213–240.

KREILOS, T., VEBLE, G., SCHNEIDER, T. M. & ECKHARDT, B. 2012 Edge states for the turbulence transition in the asymptotic suction boundary layer. *J. Fluid Mech.* arXiv:1209.0593 (submitted).

LEVIN, O. & HENNINGSON, D. S. 2007 Turbulent spots in the asymptotic suction boundary layer. *J. Fluid Mech.* **584**, 397–414.

LUNDBLADH, A. & JOHANSSON, A. V. 1991 Direct simulation of turbulent spots in plane Couette flow. *J. Fluid Mech.* **229**, 499–516.

MARIANI, P., SPALART, P. R. & KOLLMANN, W. 1993 Direct simulation of a turbulent boundary layer with suction. In *Near-Wall Turbulent Flows* (ed. R. M. C. So, C. G. Speziale & B. E. Launder), pp. 347–356. Elsevier Science.

MELLIBOVSKY, F., MESEGUER, A., SCHNEIDER, T. M. & ECKHARDT, B. 2009 Transition in localized pipe flow turbulence. *Phys. Rev. Lett.* **103**, 054502.

ROBINSON, S. K. 1991 Coherent motions in the turbulent boundary layer. *Annu. Rev. Fluid Mech.* **23**, 601–639.

SCHLATTER, P., BRANDT, L., DE LANGE, H. C. & HENNINGSON, D. S. 2008 On streak breakdown in bypass transition. *Phys. Fluids* **20**, 101505.

SCHLATTER, P. & ÖRLÜ, R. 2011 Turbulent asymptotic suction boundary layers studied by simulation. *J. Phys.: Conf. Ser.* **318**, 022020.

SCHLICHTING, H. 1987 *Boundary-Layer Theory*, 7th edn. McGraw-Hill.

SCHMID, P. J. & HENNINGSON, D. S. 2001 *Stability and Transition in Shear Flows*. Springer.

SCHNEIDER, T. M., ECKHARDT, B. & YORKE, J. A. 2007 Turbulence transition and the edge of chaos in pipe flow. *Phys. Rev. Lett.* **99**, 034502.

SCHNEIDER, T. M., GIBSON, J. F., LAGHA, M., DE LILLO, F. & ECKHARDT, B. 2008 Laminar–turbulent boundary in plane Couette flow. *Phys. Rev.* E **78**, 037301.

SCHNEIDER, T. M., MARINC, D. & ECKHARDT, B. 2010 Localized edge states nucleate turbulence in extended plane Couette cells. *J. Fluid Mech.* **646**, 441–451.

SKUFCA, J. D., YORKE, J. A. & ECKHARDT, B. 2006 Edge of chaos in a parallel shear flow. *Phys. Rev. Lett.* **96**, 174101.

SPALART, P. R. 1988 Direct simulation of a turbulent boundary layer up to $R_\theta = 1410$. *J. Fluid Mech.* **187**, 61–98.

SPALART, P. R. & YANG, K. S. 1987 Numerical study of ribbon-induced transition in Blasius flow. *J. Fluid Mech.* **178**, 345–365.

TOH, S. & ITANO, T. 2003 A periodic-like solution in channel flow. *J. Fluid Mech.* **481**, 67–76.